Control Technology Lessons Learned: Case Study Using the Micro-Precision Interferometer Testbed *

Gregory W. Neat and Alex Abramovici
Jet Propulsion Laboratory
California Institute of Technology
Pasadena, CA 91109

Abstract

The paper presents a partial account of control lessons learned during the development of the Micro-Precision Interferometer (MPI) testbed. The paper describes a number of lessons through the design, implementation and test of a specific testbed control system. However, the described lessons are not specific to the application. The topics range from global aspects like how to measure system performance to detailed compensator implementation issues. All of the insights presented would not have been reached without this hardware step.

1. System Description

This paper describes a number of control system lessons learned on a complex opto-mechanical system; the Micro-Precision Interferometer (MPI) testbed (see Figure 1 and Ref. [1]). The testbed contains over 65 actuators and over 100 sensors which are either directly part of the instrument or facilitate testing this future space structure in a ground-based laboratory. This paper discusses one of the many testbed closed loop systems; the fringe tracker control system and the significant lessons learned from the designing, implementing and testing it.

The fringe tracker control system must equalize the optical paths from the star through each arm of the interferometer to the point where they are combined. This subsystem must provide the required disturbance rejection below 10 Hz, and share responsibility with the isolation system between 10 Hz and 300 Hz. On-orbit, photon statistics associated with dim stellar targets are expected to limit fringe tracker bandwidth to a few hundred Hz. This translates into the following top-level requirements:

- Open-loop bandwidth must be less than 300 Hz.
- Loop gain up to 300 Hz should be maximized.
- Closed-loop system must have gain margin of at least 6 dB and phase margin of at least 30^o.

Figure 2 shows a block diagram of the control system implementation. The error signal for the system is an optical phase difference (fringe position). The pseudostar light source, a HeNe 633 nm laser, is located on a passively-isolated, four meter optical table. This

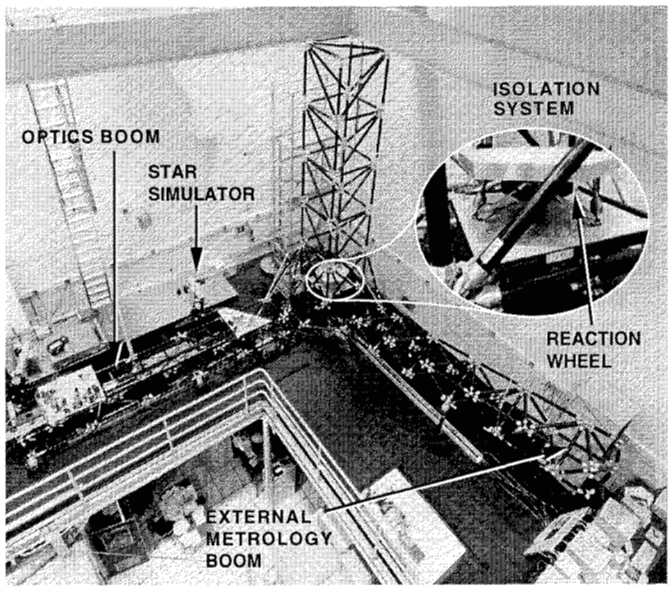

Figure 1: Bird's eye view of the MPI testbed with inset showing a close-up of the six-axis isolation system.

beam is split and directed with flat mirrors to the respective testbed collecting apertures (siderostats). The testbed is suspended from the ceiling with an active pneumatic/electromagnetic suspension system, with all suspension modes below 1 Hz. Starting with each collecting aperture the star light bounces off twelve surfaces in each interferometer arm before entering the fringe detector.

The optical phase difference is controlled by changing the optical path difference using the active delay line. Each delay line consists of a parabolic primary mirror and a flat secondary mirror. Collimated light entering the assembly exits as a collimated collimated beam parallel, vertically displaced and travelling in the opposite direction with respect to the input beam. The passive delay line is bolted to the MPI structure. The active delay line includes three actuators, each of which has a unique stroke and bandwidth. Together, these actuators introduce the commanded optical delay into one interferometer arm with the resolution and bandwidth of the small signal actua-

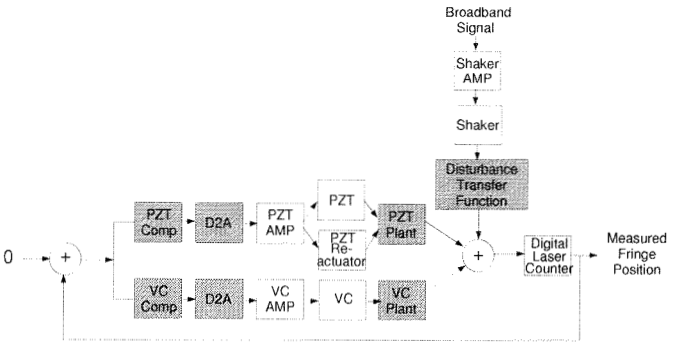

Figure 2: Block diagram of the fringe tracking control system.

tor and the dynamic range of the large stroke actuator. The three stages are: a stepper motor for low-frequency (dc), long-travel capability (1 m); a voice-coil actuator for medium-frequency (dc – 10 Hz), medium-amplitude control (1 cm); and a reactuated piezo-electric device (PZT) for high-bandwidth (up to 1 kHz), precise actuation (30μm range, sub-nanometer resolution.).

The optical assembly is attached with flexures (flexure mode: 1 Hz, parallel to the light beam) to the stepper motor driven cart. The voice-coil motor pushes the optical assembly along the degree of freedom allowed by the flexures. The PZT moves the secondary mirror within the optical assembly. A reactuator PZT is mounted in tandem with the secondary mirror PZT. Generally, the optics cart stepper motor is fixed during observations. Hence, only the voice-coil and the PZT are significant to the vibration attenuation design.

The fringe tracker control algorithm is implemented digitally on a single 68040 microprocessor and provides commands to the delay line at 8 kHz. The fringe position is measured with a custom digital laser counter board with 2.5 nm resolution.

This is a two input, one output control problem. The two actuators are configured in parallel. The control design approach assigns control authority for a specific frequency range to a specific actuator, analogously to the approach taken in Ref. [2].

Since the voice coil moves the mass of the entire optical assembly, this plant transfer function couples with structural dynamics. In contrast, the PZT is effectively decoupled from to the structure, by providing both the secondary mirror PZT and the reactuation PZT with the same command, thus cancelling the reaction forces.

Figure 2 shows the control system block diagram in terms of the PZT, voice coil, and Figure 3 shows the loop gains: L_{PZT}, L_{VC}, and L_{TOT}, respectively. The design objective is for L_{VC} to dominate at low frequency and L_{PZT} to dominate at high frequency.

Given the expected disturbance spectra, the PZT actuator dynamic range enforces a lower limit on f_{ho}. On

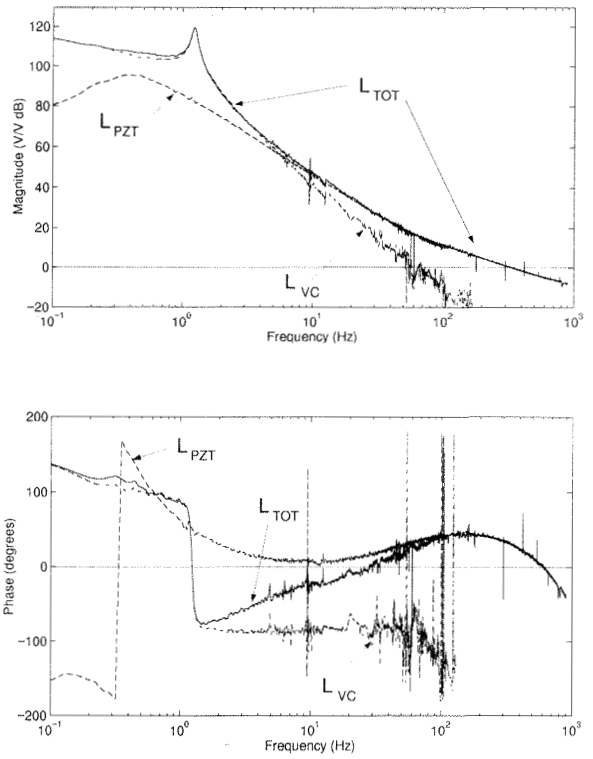

Figure 3: Fringe tracker control system loop gains (magnitude and phase).

the other hand, the influence of structural modes in the voice-coil plant transfer function reduces hand-off stability margin as the hand-off frequency is increased. Within these constraints, the hand-off frequency was chosen to be 7 Hz. Classical control design methods were used to frequency-shape the loops for maximum feedback, based on laboratory measurements of the plant transfer functions. The resulting system has an open-loop bandwidth of 300 Hz. Figure 3 indicates that the system is conditionally stable with adequate gain and phase margins.

2. How Do You Measure Performance?

Performance assessment for this control system began with a rather narrow-minded definition and ended with a rather exhaustive definition/procedure. Traditionally, loop gains or loop sensitivity funtions are used to quantify compensator performance. This metric however does not consider the spectrum of the actual disturbance to be rejected. Initial studies with this compensator were time domain step responses from open to closed loop (see Figure 4). The control system was rejecting the ambient background noise which was poorly understood (see "know your ambient environment" lesson learned).

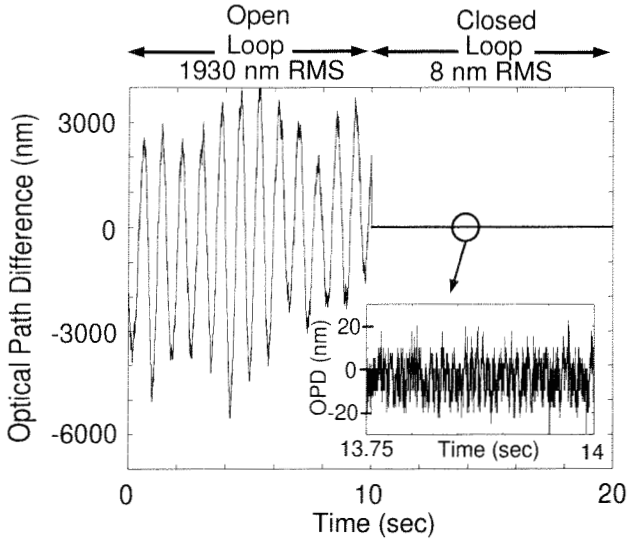

Figure 4: Optical path difference as a function of time for the fringe tracker loop open and closed.

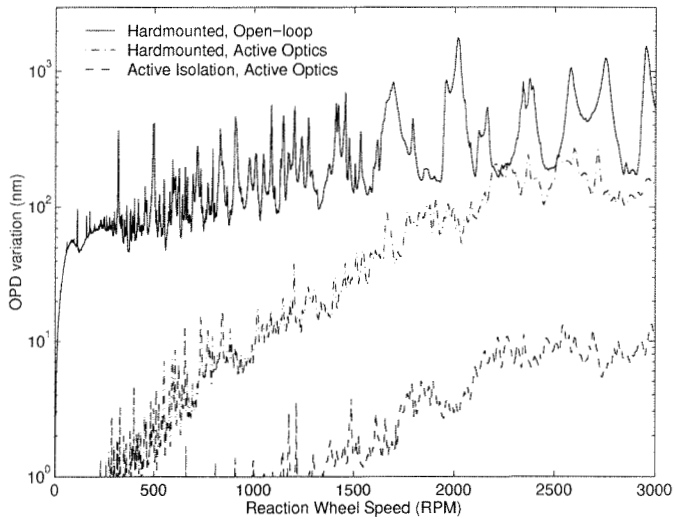

Figure 5: Optical path difference as a function of wheel speed for the fringe tracker loop open and closed.

However, this was the wrong disturbance environment to address with regard to the ultimate space application. The relevant disturbance for the on-orbit problem were narrowband forces emitted from the spacecraft reaction wheel assemblies. The nature of this on-orbit disturbance was different from the ambient environment in both magnitude and frequency. After attempting to emulate the on-orbit disturbance environment in the ground-based laboratory, unforseen constraints such as the time required to cover the range of reaction wheel disturbances and the difficulty in measuring the effect on the on-orbit vibrations above the ambient lab noise environment lead to a hybrid performance assessment approach.

The performance assessment procedure is broken into two distinct measurement procedures. In the first test, the fringe tracker compensator attempts to reject the ambient lab environmental disturbance. The level to which this is achieved demonstrates that the loop actuators, sensors and electronics can all operate at the required levels despite the fact that the disturbance does not have the correct signature. In the second test, disturbance transfer functions are measured from the reaction wheel mount location to the output metric in six degrees of freedom. Offline, an emprical model of the reaction wheel disturbance is played through these transfer functions, ultimately generating an output metric versus reaction wheel rpm plot (see Figure 5). The required stabilization must be satisfied for both tests.

The design and implementation of this performance measurement approach was a major activitiy requiring significant resources that were initially unforeseen. Figure 6 shows a summary of these two test results as a function of years we have been addressing this problem. Note that it was not until 1997 that the astrometric requirement was successfully achieved by both approaches and therefore satisfied by our performance assessment definition.

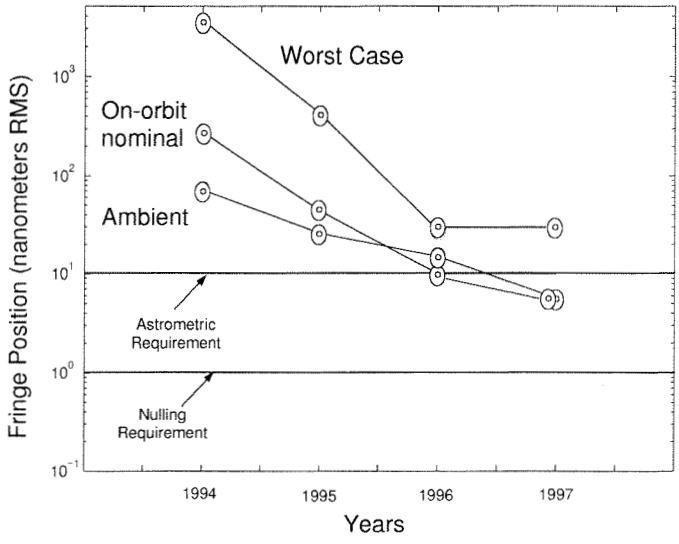

Figure 6: Fringe tracker loop performance in terms of three different metrics over the course of the last several years.

3. System Parameters Really Do Vary

Considerable effort lead to the fringe tracker loop operating reliably and with good performance, as shown in Fig. 4. Having displayed stable behavior for several months, the loop suddenly started to build up an oscillation when closed, as shown in Fig. 8.

Comparing old measurements of voice coil to OPD transfer functions with measurements taken after the un-

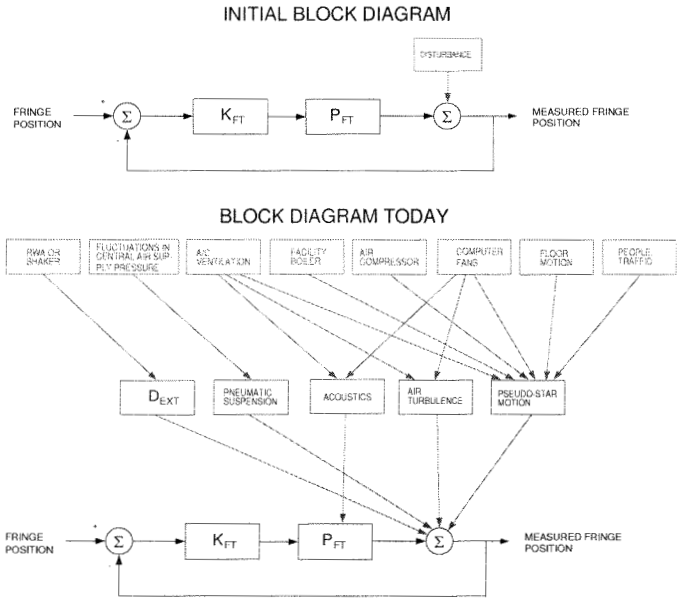

Figure 7: Understanding of interaction between the environment disturbances and the fringe tracker today, compared to four years ago.

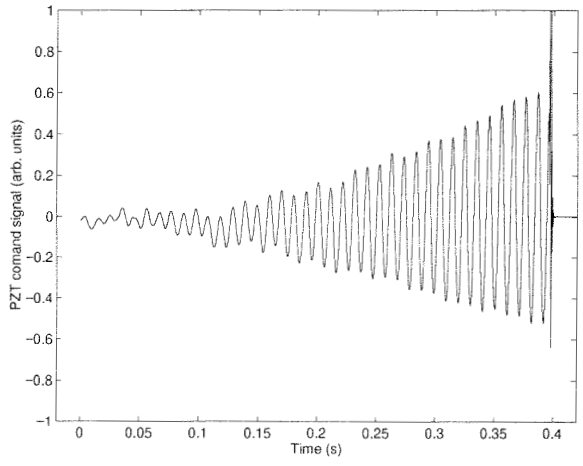

Figure 8: Time domain record of pzt command signal showing instability build-up.

stable behavior set in showed that a large split peak at 100 Hz, and a sharp peak at 70 Hz had appeared (see Fig. 9). Even though control from the voice coil is handed off to the PZT at $\sim$ 6 Hz, (Fig. 3) the peak is high enough to break above the PZT transfer function and, through its large phase distortion, cause the observed instability.

A lengthy experimental investigation located the 100 Hz resonance at the delay line voice coil mounting plate. It was further determined that several subassemblies attached to the testbed and coupled to the optical path difference were resonating at frequencies within the bandwidth of the 100 Hz peak in the voice coil transfer function, increasing the coupling of the resonance to the OPD and leading to the instability (Fig. 10). We conjectured that the resonance was always there, but at a slightly different frequency, which prevented it from exciting the subassemblies shown in Fig. 10. The problem must have occured when the mounting plate resonance shifted because of a change in some parameter, e. g. the tightness of a fastener. The immediate solution consisted of detuning the resonance by clamping a piece of metal to the voice coil mounting plate. The permanent solution called for a thicker mounting plate.

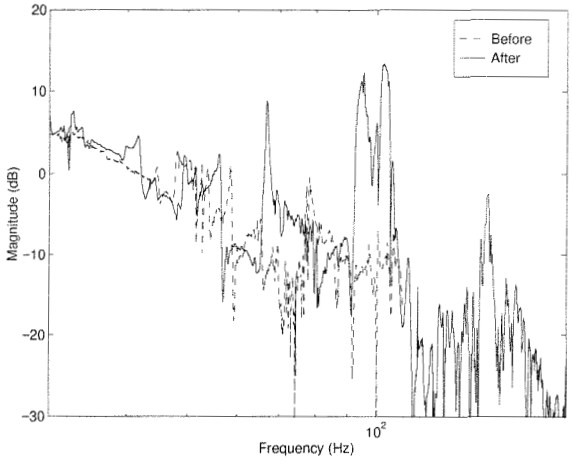

Figure 9: Comparison of voice coil transfer functions before and after malfunction.

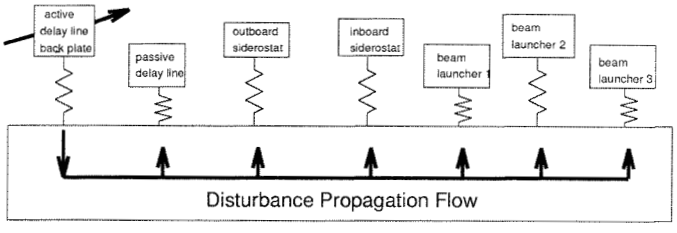

Figure 10: Disturbance propagation flow through MPI structure.

Lessons learned

- This problem could have only been discovered with a testbed. No model with realistic fidelity would have predicted this. The MPI high fidelity model describes the delay line only as a 1 Hz pendulum with the correct mass.

- System level design should be alert to the stacking up of component modes.

Acknowledgments

The research described was performed at the Jet Propulsion Laboratory of the California Institute of Technology, under contract with the National Aeronautics and Space Administration. The authors thank the leaders of the Interferometer Technology Program, Bob Laskin, Jeffrey Yu, and Ben Parvin for their technical and financial support.

References

[1] G. W. Neat, A. Abramovici, J. M. Melody, R. J. Calvet, N. M. Nerheim, and J. F. O'Bien, "Control Technology Readiness for Spaceborne Optical Interferometer Missions", The Space Microdynamics and Accurate Control Symposium, Toulouse, France, May, 1997

[2] J.T. Spanos, Z. Rahman, C. Chu, and J.F. O'Brien, "Control Structure Interaction in Long Baseline Space Interferometers," 12th IFAC Symposium on Automatic Control in Aerospace, Ottobrunn, Germany, September 7-11, 1992.